Influence of disorder on the structural phase transition and magnetic interactions in Ba3−xSrxCr2O8

Grundmann, Henrik ; Schilling, Andreas ; Medarde, Marisa ; Sheptyakov, Denis

DOI: https://doi.org/10.1103/PhysRevB.90.075101

Influence of disorder on the structural phase transition and magnetic interactions in $Ba_{3-x}Sr_xCr_2O_8$

Henrik Grundmann* and Andreas Schilling

Physik-Institut, Universität Zürich, Winterthurerstrasse 190, CH-8057 Zürich

Marisa Medarde

Laboratory for Development and Methods,

Paul Scherrer Institut, 5232 Villigen PSI, Switzerland

Denis Sheptyakov

Laboratory for Neutron Scattering, Paul Scherrer Institut, 5232 Villigen PSI, Switzerland

(Dated: July 2, 2014)

Abstract

The magnetic intradimer interaction constant J_0 in the spin dimer system $Ba_{3-x}Sr_xCr_2O_8$ can be tuned by varying the Sr content x. Very interestingly, this variation of J_0 with x is highly nonlinear. In the present study, we show that this peculiar behavior of J_0 can be only partly explained by the changes in the average crystal structure alone. We report on neutron powder diffraction experiments to probe the corresponding structural details. Performing extended Hückel tight binding calculations based on those structural details obtained at liquid helium temperatures, we found that the change of the magnetic interaction constant can be well reproduced by taking into account the presence of a structural transition due to the Jahn-Teller active Cr^{5+}-ions. This transition, lifting the orbital degeneracy and thereby the magnetic frustration in the system, is heavily influenced by disorder in the system arising from partially exchanging Ba with Sr.

I. INTRODUCTION

Bose-Einstein-condensation (BEC) is one of the most fascinating aspects in modern physics. A decade ago, the field of spin dimer physics has been closely linked to this topic by explaining several properties of certain spin dimer systems in terms of a BEC of magnetic quasiparticles (triplons)[1]. The triplons, formed by dimers of magnetic ions, condense at a low enough temperature T and above a critical magnetic field $H_c(T)$. Once the condensate is formed, the triplons should show macroscopic phase coherence, a defining property of every BEC. It has very recently been suggested that this phase coherence could be probed in a device of two coupled spin dimer materials with different critical fields[2], which would represent a direct analogue to a Josephson junction showing the a.c.-Josephson effect. As in superconductors and atomic BEC's[3,4], this effect is based on the existence of a phase coherent macroscopic wave function. A successful detection of Josephson effects in spin dimer systems would therefore be a direct proof for macroscopic phase coherence and allow to classify the observed spin condensate as a true BEC.

As the above sketched experiment requires two spin systems with a certain difference in the respective critical fields H_c, the fine tuning of this parameter becomes necessary. The critical field largely depends on the intradimer magnetic interaction constant J_0 between the ions that form the spin dimers. The J_0 is essentially determined by the specific (super-)exchange path between those ions and therefore changes if the crystal structure is modified. The spins systems $Ba_3Cr_2O_8$ and $Sr_3Cr_2O_8$, two candidates for a triplon BEC[5–7], represent such spin systems with a similar structure, but strongly differing magnetic interactions. For the corresponding mixed system $Ba_{3-x}Sr_xCr_2O_8$, J_0 has been reported to be tunable in a non-linear way[8] by changing the Sr content x, but it was found to change in a peculiar, non-monotonous way as a function of x which contrasts with the almost linear changes of the lattice parameters. Up to now, this discrepancy has not been resolved.

The present work aims to give a satisfactory explanation based on a more detailed examination of changes in the crystal structure with x. It has been shown for $Sr_3Cr_2O_8$ that due to a Jahn-Teller type, temperature induced structural phase transition involving certain oxygen positions (which is present for both $Ba_3Cr_2O_8$ and $Sr_3Cr_2O_8$), J_0 is strongly enhanced at at low temperatures[9]. Using neutron powder diffraction techniques which are more sensitive to the oxygen positions than corresponding X-ray diffraction data in the

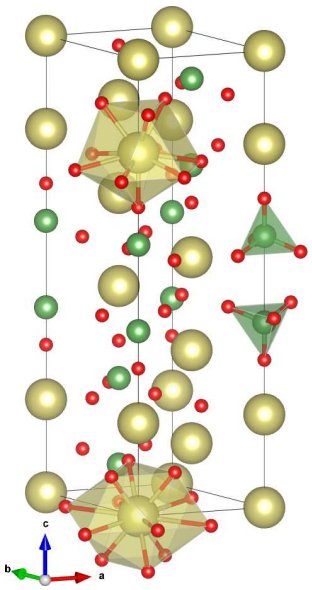

FIG. 1. Crystal structure of $Ba_{3-x}Sr_xCr_2O_8$ at room temperature. The Cr-tetrahedron is shown in dimer configuration on the right, the Ba_1/Sr_1-dodecatope is shown on the bottom and the Ba/Sr_2-decatope is shown on the top of the drawing. Large spheres:Ba/Sr, medium spheres: Cr, small spheres: O.

presence of heavy elements such as Sr and Ba, we have investigated the crystal structure of $Ba_{3-x}Sr_xCr_2O_8$ for several values of x at room temperature and at $T = 2\,\mathrm{K}$. Based on the obtained lattice parameters and atomic positions, we performed extended Hückel tight binding (EHTB) calculations to estimate J_0 as a function of x.

II. EXPERIMENTAL DETAILS

Synthesis

The polycrystalline samples were prepared by standard solid state reaction schemes. Powders of $BaCO_3$ (99,98%, *Sigma-Aldrich*), $SrCO_3$ (99,9%, *Sigma-Aldrich*) and Cr_2O_3 (99,9%, *Sigma-Aldrich*) were mixed according to

$$(3-x)\mathrm{BaCO_3} + x\mathrm{SrCO_3} + \mathrm{Cr_2O_3} \rightarrow \mathrm{Ba_{3-x}Sr_xCr_2O_8} + \mathrm{CO_n},$$

ground and heated in flowing Ar at 1300 °C. The heating was started with a linear ramp up to 1300 °C in 5 h. The samples remained at this temperature for 12 h, followed by a

linear cooling to room temperature in 8 h. The grinding at heating was repeated twice. We prepared samples with $x \in \left\{0, \frac{1}{3}, \frac{2}{3}, 1, \frac{4}{3}, \frac{5}{3}, 2, \frac{7}{3}, \frac{8}{3}, 3\right\}$.

A. Neutron Diffraction

The neutron powder diffraction experiments were carried out at the HRPT[10] at Paul-Scherrer-Institute (PSI, Villigen) at room temperature and at $T = 2\,\mathrm{K}$, using $\lambda = 1.494\,\text{Å}$ [Ge(533)]. Scans were performed with fixed primary soller collimation (40') and a secondary slit of (40'). The powder samples ($\approx$ 6 g) were loaded into cylindrical vanadium containers of 8 mm diameter (6 mm for $Ba_{\frac{8}{3}}Sr_{\frac{1}{3}}Cr_2O_8$). The low temperature measurements were performed using a He cryostat, whose contribution to the total scattering was minimized using an oscillating radial collimator. The obtained diffractograms were analyzed using the Rietveld package emphFullProf suite (available free of charge at http://www.ill.eu/sites/fullprof/.).

Tight binding calculations

Based on these structure data, we calculated the antiferromagnetic interaction constant J_0 using the extended Hückel tight binding method which was successfully used in the past to estimate the interaction constants in $Ba_3Cr_2O_8$[11] and $Sr_3Cr_2O_8$[9]. These calculations are based on determining the orbital splittings $\Delta e_{\mu\mu}$ of the occupied chromium orbitals. This splitting $\Delta e_{\mu\mu}$ of the μ-th considered orbital occurs when two CrO_4^{6-}-tetrahedra are brought together to form a dimer (see Fig. 2) and it can be calculated directly. Based on these splittings, J_0 can be estimated as $J_0 = \frac{\langle(\Delta e)^2\rangle}{U}$, where U is a repulsion potential and $\langle(\Delta e)^2\rangle = \frac{1}{n}^2 \sum_{\mu}(\Delta e_{\mu\mu})^2$ is a sum over all n occupied orbitals. Due to the degeneracy of the $3z^2 - r^2$- and the $x^2 - y^2$-orbital at room temperature, both orbitals have to be taken into account when calculating $\langle(\Delta e)^2\rangle$. At temperatures below the Jahn-Teller transition, however, only the $3z^2 - r^2$ orbital is occupied (see below), so that $\langle(\Delta e)^2\rangle = (\Delta e_{3z^2-r^2})^2$. A more detailed description of the general implementation of this procedure and its limitation to antiferromagnetical interactions can be found in[12]. The ETHB calculations have been performed using the *SAMOA*-suite (available free of charge at http://www.primec.com/.).

The repulsion potential U depends on the chemical composition and should vary gradually

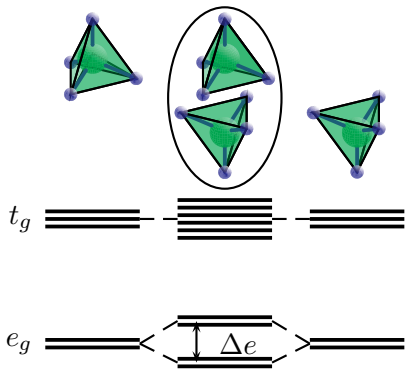

FIG. 2. Sketch for the orbital splitting Δe that occurs when two CrO_4^{3-}-tetrahedra form a dimer. The sketch refers to the undistorted structure.

with the Sr concentration x[13]. Assuming a linear behavior as a function of x, $U(x) = A{\cdot}x{+}B$, we calculated $J_0(x)$ from $J_0 = \frac{\langle \Delta e \rangle^2}{A \cdot x + B}$. Values for A and B were determined by comparing the published experimental values of J_0 (from inelastic neutron scattering)[14,15] with the calculated orbital splitting for the considered compounds in the low temperature phase.

III. RESULTS AND DISCUSSION

In the neutron powder diffraction patterns obtained at room temperature, the observed Bragg reflections could be indexed using the space group $R\bar{3}m$ for all x. From the Rietveld refinement of the diffraction data we obtained an almost linear behavior of the lattice constants a and c as a function of the Sr content, in accordance with recently reported X-ray diffraction experiments (see Fig. 3).

Our analysis of the diffraction patterns obtained at $T = 2\,\mathrm{K}$ shows that the lattice symmetry is lowered for some, but not all values of x upon cooling. For chemical compositions close to the parent compounds, i.e. for $x \in \{0, 0.33, 2.33, 3\}$, the lattice is better described using the space group $C_{2/c}$, that has been reported for $Ba_3Cr_2O_8$ and $Sr_3Cr_2O_8$, with new diffraction peaks appearing (see Fig. 4). For the remaining samples, no superstructure peaks could be observed. The diffraction pattern at $T = 2\,\mathrm{K}$ could be well described by the room temperature space group $R\bar{3}m$, indicating a suppression of the structural phase transition for the samples with $0.33 < x < 2.33$.

Where detected, the symmetry breaking is due to a horizontal displacement δs of the

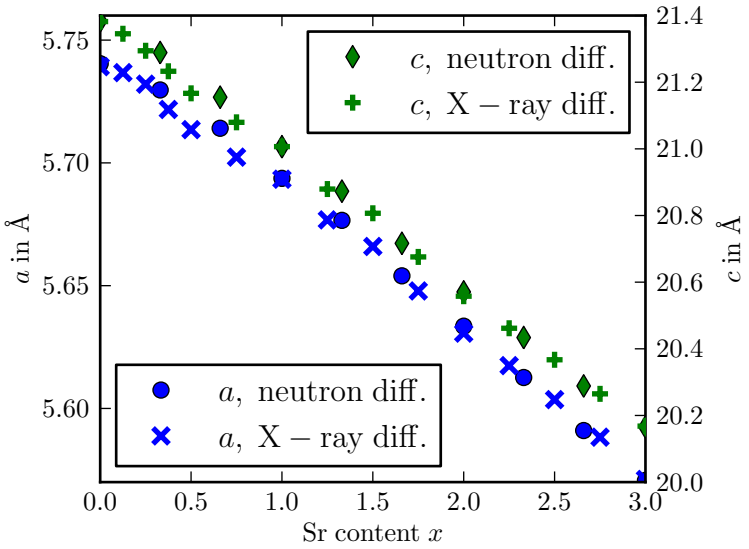

FIG. 3. Lattice constants a and c of $Ba_{3-x}Sr_xCr_2O_8$ at room temperature (space group $R\bar{3}m$). The lattice constants are shown as a function of the Sr content x as obtained from X-ray[8] and neutron powder diffraction experiments. The error bars for the values obtained from neutron diffraction are smaller than the size of the markers.

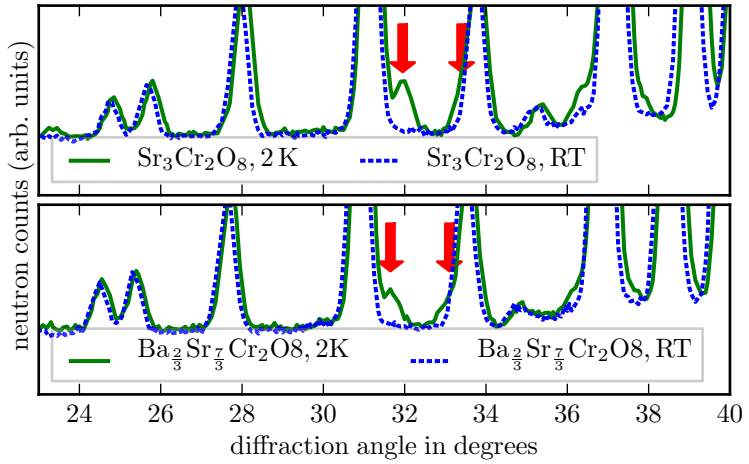

FIG. 4. Additional peaks appearing in the low temperature neutron diffractograms for $Sr_3Cr_2O_8$ and $Ba_{\frac{2}{3}}Sr_{\frac{7}{3}}Cr_2O_8$, indicating the structural phase transition.

apical oxygen in the tetrahedron surrounding the Cr^{5+}-ions (O_1 in our notation, see Figs. 1 and 6). As shown in Fig. 6, this δs is smaller for intermediate x than for the parent compounds. By shifting O_1 along the O_2-O_3-edge, the site symmetry of the Cr-ions ($3m$ at room temperature) is lost. This oxygen shift affects the electronic orbitals of the Cr-ions.

In the case of a perfect tetrahedron, the d-orbitals are grouped into a lower lying, twofold degenerate e_g state and a higher lying, threefold degenerate t_g state. When the symmetry breaking occurs in $Ba_{3-x}Sr_xCr_2O_8$, the e_g state degeneracy is lifted, with a separation into a lower lying $3z^2-r^2$ orbital and a higher lying x^2-y^2 orbital. Therefore, both of the e_g-states have to be considered when calculating $\langle \Delta e \rangle$ in case of the space group $R\bar{3}m$, whereas only the $3z^2 - r^2$ orbital has to be taken into account for $C_{2/c}$.

To quantitatively examine the effect of the oxygen shift on the interaction constant J_0, we calculated the energy splitting $\langle \Delta e \rangle$ for the obtained crystals structures and estimated the repulsion potential U. Unfortunately, no experimental values for J_0 at room temperature have been reported. To obtain reasonable values for U, we therefore first carried out ETHB calculations based on the low temperature structures for $x = 0$ and $x = 3$. For the occupied $3z^2-r^2$, our calculations calculations yielded orbital splitting energies $\Delta e(x = 0) = 5.6\,\mathrm{meV}$ and $\Delta e(x = 0) = 3.9\,\mathrm{meV}$. From these values and the reported interaction constants $J_0^{\mathrm{Ba}} = 2.38\,\mathrm{meV}$[14] and $J_0^{\mathrm{Sr}} = 5.55\,\mathrm{meV}$[15], we obtained $A = -216\,\mathrm{meV}$ and $B = 648\,\mathrm{meV}$. Based on these parameters, we could estimate the value of repulsion potential U for all examined values of x. As we assumed U to be temperature independent, the same values of $U(x)$ were used to calculate for J_0 at low temperature and at room temperature from the calculated splittings $\langle \Delta e \rangle$.

In Fig. 5, we have plotted the previously reported values of J_0 as obtained from fitting magnetization data $M(T)$ together with the results of our calculations of J_0 at room temperature and at $T = 2\,\mathrm{K}$. These experimental J_0 values are most sensitive to the low-temperature magnetization part of the $M(T)$ data used for the fitting procedure. Therefore, they are valid well below room temperature. Fig. 5 demonstrates, as expected, that the experimental values can be well reproduced within the ETHB framework if the corresponding calculations are based on the low temperature structure. By contrast, the calculated room temperature values of J_0 underestimate the experimental values for a wide range of x. On the other hand, the experimental values and the calculations for both the room temperature and low temperature structure almost coincide for a Sr content of $x \approx 1.33$. For this composition, our neutron diffraction experiments did not indicate any evidence for the structural symmetry breaking that we observed for the other values of x at $T = 2\,\mathrm{K}$. Furthermore, combining the results of Figs. 6 and 5, suggests that a larger value of J_0 seems to be accompanied by a stronger symmetry breaking.

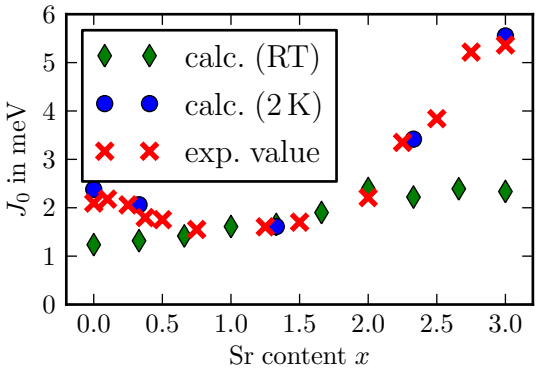

FIG. 5. Intradimer interaction constant J_0 for $Ba_{3-x}Sr_xCr_2O_8$ as a function of the Sr content x. The shown data points are experimentally obtained from SQUID-measurements and estimated based on EHTB-calculations for the crystal structure at room temperature and $T = 2\,\mathrm{K}$, respectively.

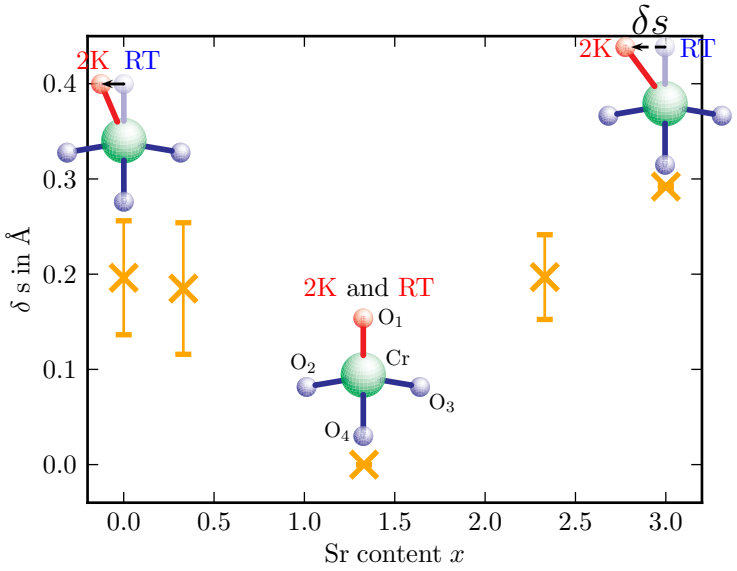

FIG. 6. Distance δs of the apical oxygen atom from the dimer axis as a function of the Sr content x. The distance in the corresponding sketches is exaggerated for visual clarity.

From these results, we conclude that the Jahn-Teller distortion, which induces an orbital ordering[9,11], increases the intradimer interaction constant J_0 for $0 < x < 3$, as it was reported for $Sr_3Cr_2O_8$. Without this orbital ordering, the splitting $\langle \Delta e \rangle$ for a given x remains almost constant for all temperatures. We predict that no (or just a minimal) distortion will be present for stoichiometries for which the experimental value of J_0 is close to the calculated room temperature value.

In order to find a satisfactory explanation for the suppression of the Jahn-Teller-Distortion for intermediate values of x, which might by influenced by non-monotonous changes in the structural parameters, we examined the oxygen surroundings of the metal ions at room temperature in more detail. The oxygen tetrahedron around the Cr-ion is only slightly affected by varying the stoichiometry. Neither the tetrahedron height h_3 nor the edge length M of the base triangle change significantly as a function of x (see Fig. 7). This is reflected in the small change of the interaction constant at room temperature (see Fig. 5). This change of J_0 is mostly given by the shrinking separation of the two tetrahedra forming a dimer as a function of x.

The Ba/Sr atoms are located at two different positions (sites Ba_1 and Ba_2). The respective Wyckoff positions are $3a$ and $6c$ for R$\overline{3}$m ($4e$ and $8f$ for $C_{2/c}$). The atoms located in the Ba_2-position with point site symmetry $3m$ are 10-fold coordinated. The height h_2 of the decatope changes linearly as a function of x (see Fig. 7). The planar oxygen hexagon surrounding the Ba_2 position is not evenly formed. Although the inner angle is always $\alpha = 120°$, the edge M that is shared with the chromium tetrahedron is shorter than the edge N that is shared only with the Ba_1 dodecatope. The value of N decreases with increasing x until M and N are equal for $x = 3$ (see Fig. 7).

The position Ba_1 is twelve-fold coordinated with site symmetry $\overline{3}m$ (see Fig. 7 a). As stated above, the edge length N is shared with the Ba_2-decatope. Both edge lengths N and O as well as the dodecatope height h_1 decrease linearly as a function of x (see Fig. 7). Based on the bond lengths derived from the structural data, we have calculated the bond valence sums for Ba and Sr for both positions. These calculations were performed according to[16] and[17] and the results are plotted in Fig. 8. For both Ba/Sr-positions the average valence is almost equal to 2 for all x.

All oxygen polyhedra and corresponding ion valences therefore change strictly monotonously as a function of x, again providing no obvious reason for a suppressed Jahn-Teller distortion for intermediate values of x. The site occupancies, on the other hand, are found to be non-monotonous (see Fig. 9 and the supplementary tables). In panel b) of Fig. 9 we have plotted the probability for a given Ba-ion to occupy either site 1 or site 2 as a function of the Sr content x. As site 1 has a multiplicity of 3 and site 2 has a multiplicity of 6, the occupation probabilities should be $\frac{1}{3}$ and $\frac{2}{3}$, respectively. However, the probability for a Ba-ion to occupy site 1 increases for increasing Sr content, while that of site 2 decreases

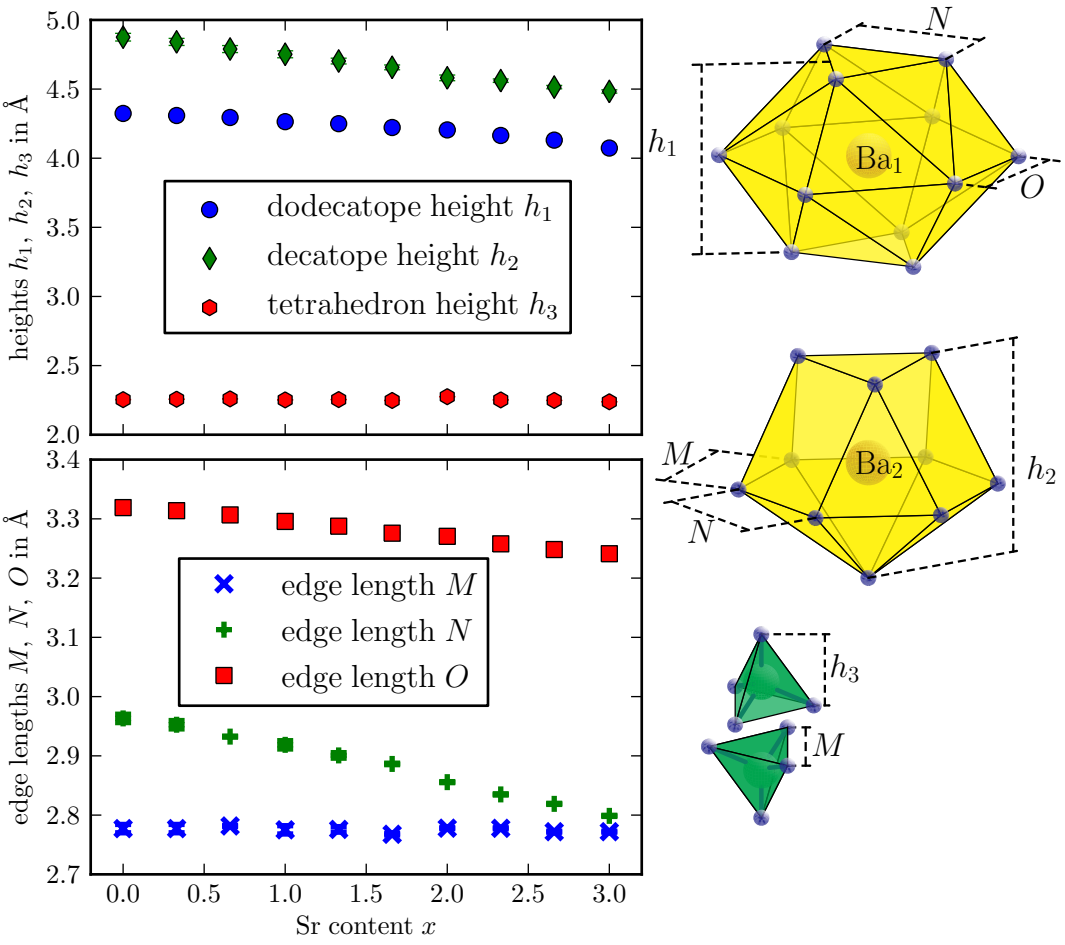

FIG. 7. Height and edge length of the oxygen polyhedra in $Ba_{3-x}Sr_xCr_2O_8$ as functions of the Sr content x. The sketches on the right show the definitions of the plotted parameters.

until both probabilities are $\approx \frac{1}{2}$. The corresponding probabilities for a given Sr-ion change accordingly. The different preferences of Sr and Ba for site 1 and site 2 can be understood by examining the calculated ion valences at both sites. As the optimal valence for Ba and Sr is 2, occupying a position where the valence would deviate from this value should require additional energy. We can therefore associate an energy $E_i^{\mathrm{Ba,Sr}} \propto \left|v_i^{\mathrm{Ba,Sr}} - 2\right|$ with valence values ν_i differing from the optimal value at site i. The energy difference $\Delta E_{i\to j}^{\mathrm{Ba,Sr}} = E_i^{\mathrm{Ba,Sr}} - E_j^{\mathrm{Ba,Sr}}$ then represents the energy gain (loss) when bringing a certain ion from site i to site j. For a positive value of $\Delta E_{i\to j}^{\mathrm{Ba,Sr}}$, site j should be preferentially occupied. In Fig. 9c, we have plotted $\Delta E_{2\to 1}^{\mathrm{Ba}}$ and $\Delta E_{1\to 2}^{\mathrm{Sr}}$ as functions of x. As both position changes are energetically favorable, site 1 should be preferred by Ba-ions and site 2 should be preferred by Sr ions, exactly as our data indicate.

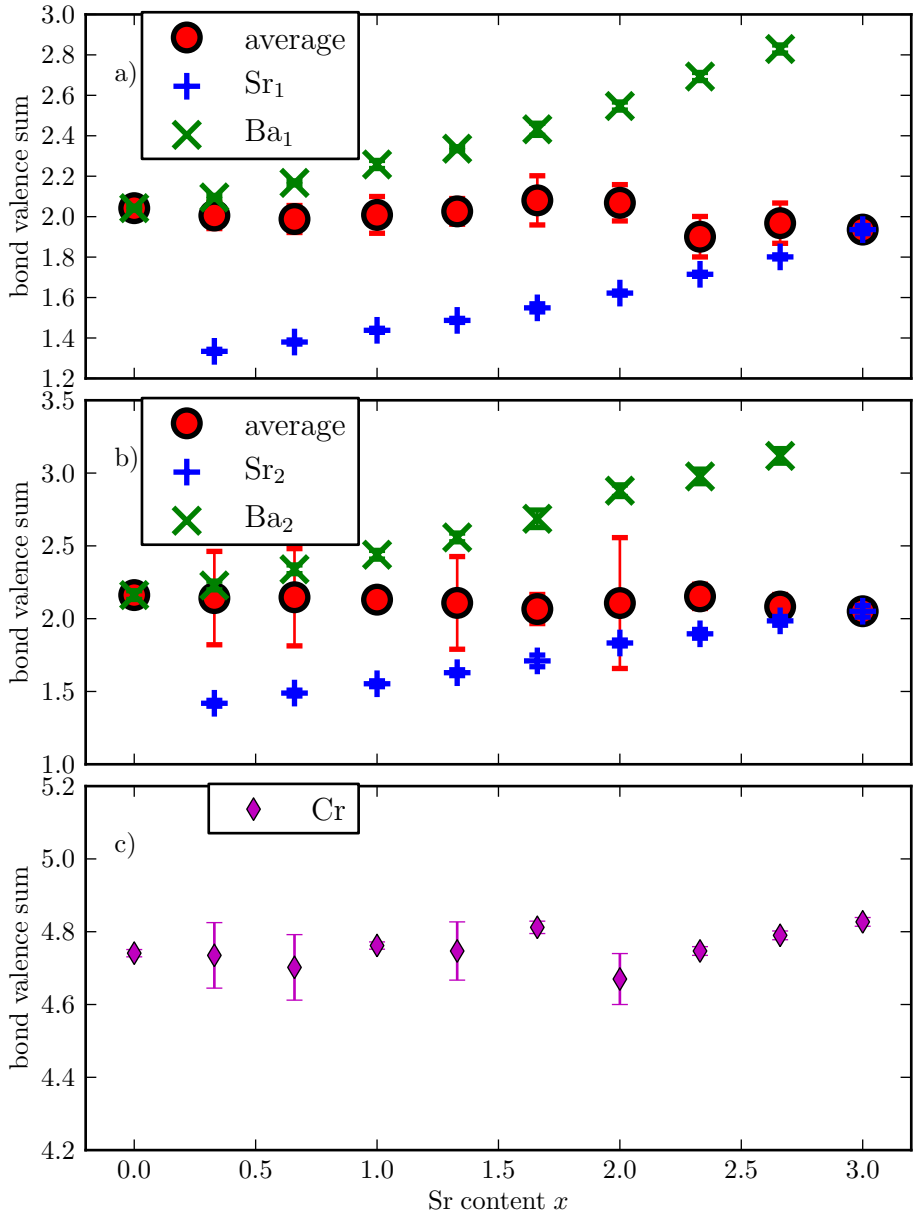

FIG. 8. Calculated bond valence sums for the Cr-ions (bottom) and the Ba/Sr-ions at sites 1 (top) and 2 (middle) in $Ba_{3-x}Sr_xCr_2O_8$ at room temperature. The average is the sum of the individual valence values weighted by the respective site occupancies.

Nevertheless, these site preferences do not directly break the site symmetry of the Cr^{5+}-ions, so that a Jahn-Teller distortion could still be energetically favorable. As shown in Fig. 8, the average bond valence sums for both Ba sites are 2+ for all studied compositions. This means that the average Ba-O distance is also nearly constant for both sites. If the mean square displacement of this average was constant, a substitution of Ba by Sr would

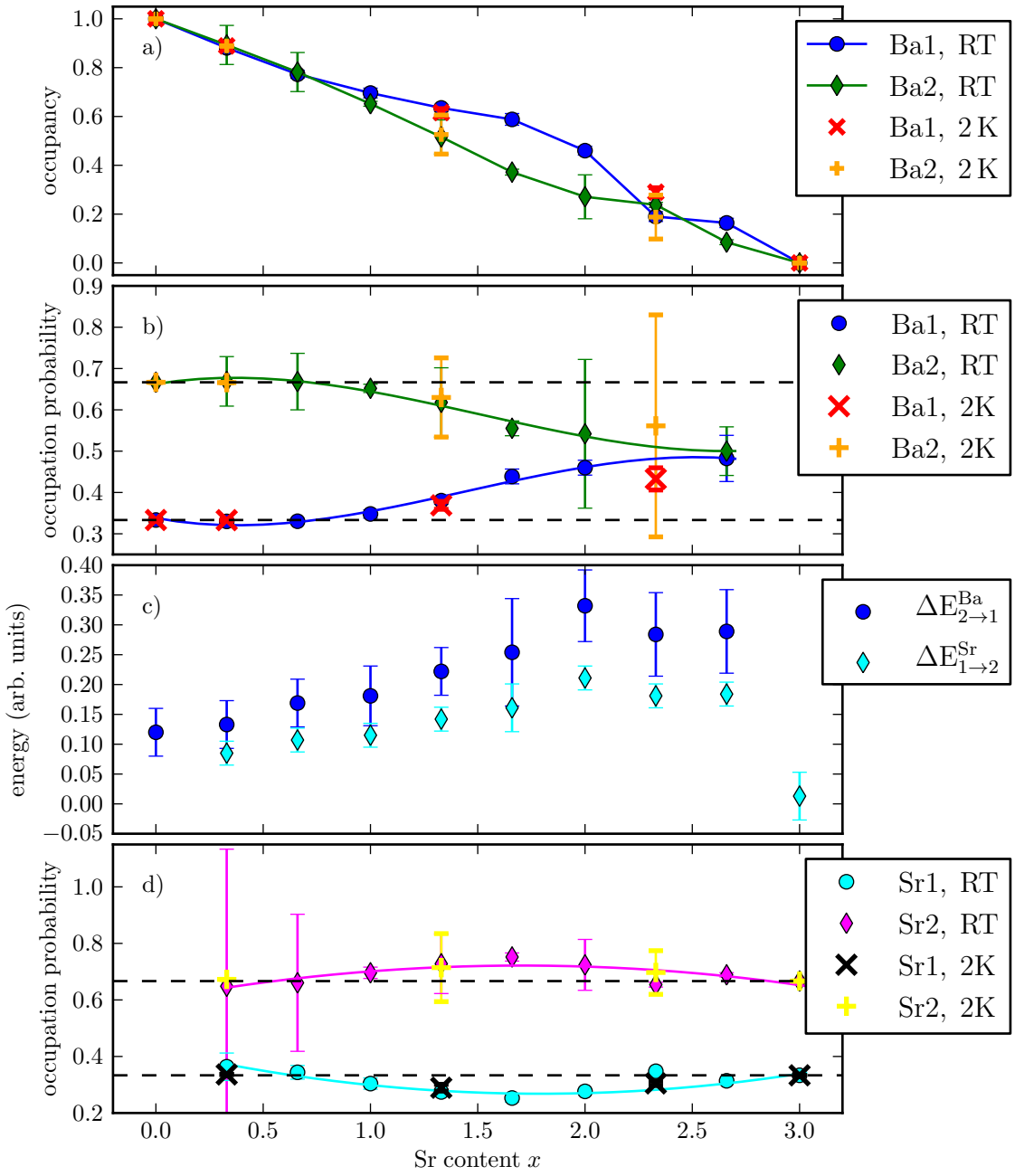

FIG. 9. a): Obtained occupancy for a for the Ba atoms at sites 1 and 2. b): Obtained probability for a given Ba-ion to occupy one of the possible atomic positions, calculated based on the values shown in panel a). c): Energy difference $\Delta E^{\mathrm{Ba}}_{2\bar{1}}$ when transferring a Ba-ion from position 2 to position 1 and the opposite for a Sr-ion. c): Probability for a given Sr-ion to occupy one of the possible atomic positions. Dashed lines mark the probability that would be expected for completely random distributions and considering the respective position multiplicities. Solid lines are cubic fits to guide the eye.

have no effect on the local symmetry of the Cr^{5+} ions, and in particular on the Jahn-Teller distortion. However, due to the very different ionic radii of Ba^{2+} and Sr^{2+}, we can expect strong local deviations from the average. This is confirmed by the variation of the mean square displacements $\langle u^2 \rangle$ as deduced from the structural refinement and shown in Fig. 10, which are found to be maximum for intermediate values of x. We attribute this behavior to an increase of the local disorder as it is common in for solid solutions. To obtain an estimate for this disorder contribution, we have assumed that u comprises a thermal and a disorder term, $u = u_T + u_D$, with no correlation between u_T and u_D. Therefore, the total mean displacement would be $\langle u^2 \rangle = \langle u_T^2 \rangle + \langle u_D^2 \rangle + 2 \langle u_D u_T \rangle = \langle u_T^2 \rangle + \langle u_D^2 \rangle$. We have assumed the thermal part to be linear in x, $\langle u_T^2 \rangle (x) = \rho x + \tau$, and calculated the corresponding values for ρ and τ based on $\langle u^2 \rangle$ for $x = 0$ and $x = 3$. We subtracted this thermal part from the experimentally obtained displacements and plotted the resulting $\langle u_D^2 \rangle (x)$ in Fig. 11. We believe that it is this type of that disorder is responsible for suppressing the Jahn-Teller induced structural phase transition. While for pure $Ba_3Cr_2O_8$ and $Sr_3Cr_2O_8$, all Cr-O distances are well defined, the different distributions of Sr/Ba-ions inside the unit cell lead to an increasing width of the distribution of Cr-O distances for intermediate values of x. The symmetry at the Cr-site is therefore broken locally and preserved only on average. This symmetry breaking lifts the degeneracy of the e_g state by an energy difference $\Delta E(x)$. As $\Delta E(x)$ increases, the possible energy gain of the phase transition is lowered and therefore this transition itself is gradually suppressed.

Interestingly, $\langle u_D^2 \rangle (x)$ is not symmetric with respect to $x = 1.5$, as it would be expected for entirely random distributions, but seems to be shifted slightly to smaller values of x. This could be due to the changing occupation probabilities for large values of x. Any deviation from a completely random distribution, i.e. any difference between the dashed lines and the experimental values in the corresponding panel *b)* of Fig. 9, would lower the total disorder (related to the Shannon entropy in[18]). As the difference is stronger for larger values of x, the observed asymmetry could indeed be induced by the changing occupation probabilities for the different sites. However, the decreasing total Ba-concentration for large values of x decreases the influence of the changing Ba-occupation probabilities. Our experimental sensitivity with respect to the atomic displacements and site occupancies is, however, not sufficient to unambiguously confirm this explanation for the observed asymmetry of $\langle u_D^2 \rangle (x)$.

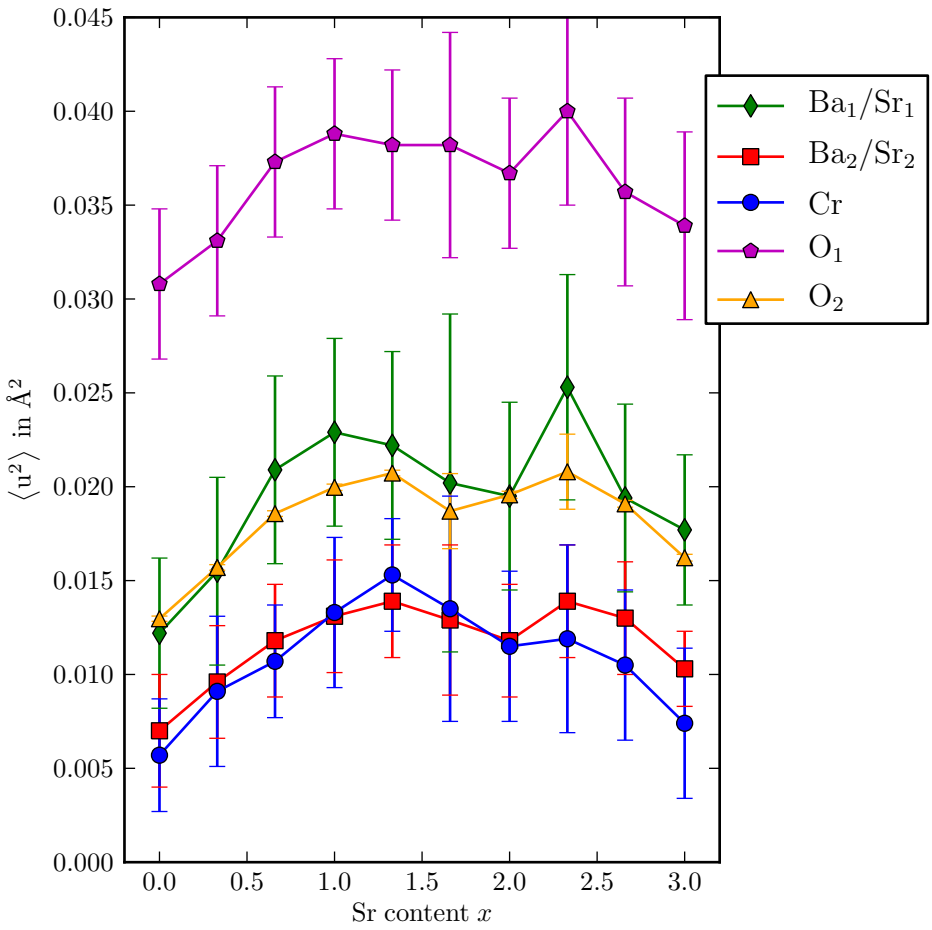

FIG. 10. Atomic displacements $\langle u^2 \rangle$ in $Ba_{3-x}Sr_xCr_2O_8$ at room temperature as a function of the Sr content x.

SUMMARY AND OUTLOOK

We have performed neutron powder diffraction experiments to obtain detailed structural information about $Ba_{3-x}Sr_xCr_2O_8$ for various values of x at room temperature and $T = 2\,\mathrm{K}$. Based on these diffraction experiments, we have shown that the Jahn-Teller distortion reported for the parent compounds is present in $Ba_{3-x}Sr_xCr_2O_8$, but seems to be gradually suppressed for intermediate values of x. We have given an explanation for this suppressed symmetry breaking at intermediate values of x based on an increasing disorder in the system. To test our hypothesis, experiments to directly probe the Cr-states as a function of the Sr content x would be extremely helpful. Furthermore, DFT-calculations of the total energy per unit cell for the two possible space groups, similar to[19], could clarify whether or not

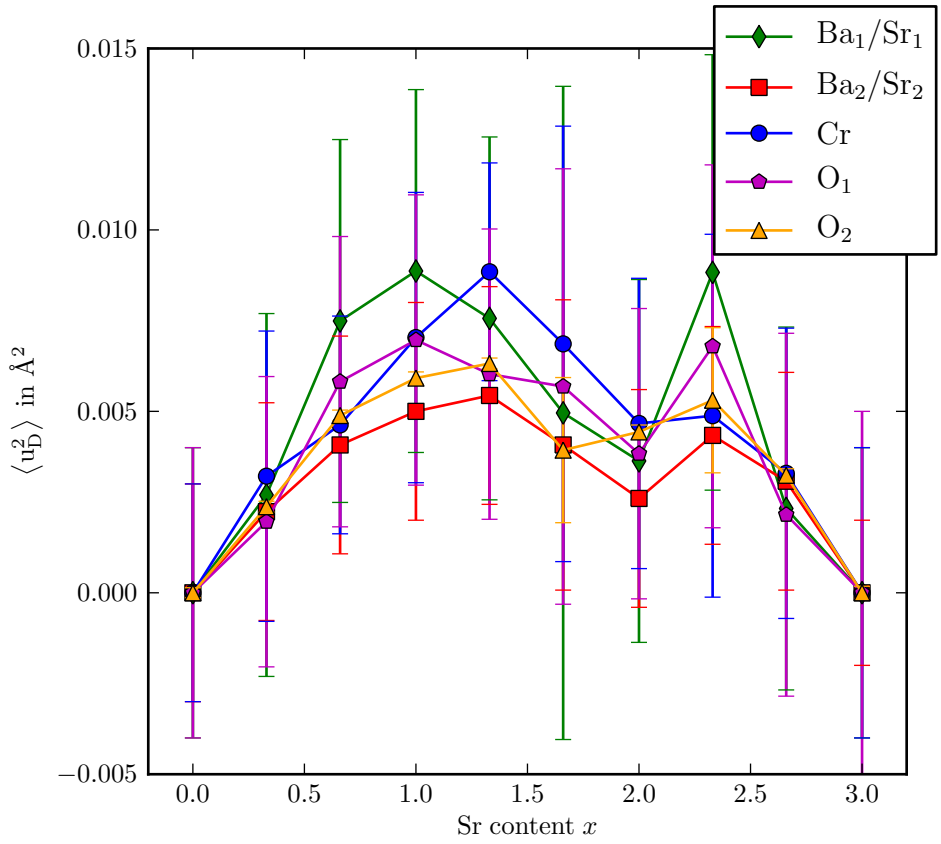

FIG. 11. Estimated disorder contribution to the atomic displacements, $\langle u^2 \rangle$, in $Ba_{3-x}Sr_xCr_2O_8$ at room temperature as a function of the Sr content x.

any symmetry breaking should be present in a disorder free system with the respective equilibrium crystal structures for intermediate values of x. We have demonstrated that the interdimer interaction constant J_0 can be calculated within the EHTB framework. We furthermore showed that the reported, peculiar change of J_0 can be explained based on the varying strength of this Jahn-Teller distortion. The tuning of J_0 with varying x as reported here should, along with a corresponging variation of the other relevant interaction constants, allow for a direct control of the critical fields H_c in the $Ba_{3-x}Sr_xCr_2O_8$ system.

---

* grundmann@physik.uzh.ch

[1] T. Nikuni, M. Oshikawa, A. Oosawa, and H. Tanaka, Phys. Rev. Let. **84**, 5868 (2000).

[2] A. Schilling and H. Grundmann, Ann. of Phys. **327**, 2309 (2012).

[3] M. Albiez, R. Gati, J. Fölling, S. Hunsmann, M. Cristiani, and M. K. Oberthaler, Phys. Rev. Lett. **95**, 010402 (Jun 2005).

[4] S. Levy, E. Lahoud, I. Shomroni, and J. Steinhauer, Nature **449**, 579 (Oct 2007).

[5] A. A. Aczel, Y. Kohama, M. Jaime, K. Ninios, H. B. Chan, L. Balicas, H. A. Dabkowska, and G. M. Luke, Phys. Rev. B **79**, 100409 (Mar 2009).

[6] A. A. Aczel, Y. Kohama, C. Marcenat, F. Weickert, M. Jaime, O. E. Ayala-Valenzuela, R. D. McDonald, S. D. Selesnic, H. A. Dabkowska, and G. M. Luke, Phys. Rev. Lett. **103**, 207203 (Nov 2009).

[7] D. Kamenskyi, J. Wosnitza, J. Krzystek, A. Aczel, H. Dabkowska, A. Dabkowski, G. Luke, and S. Zvyagin, Journal of Low Temperature Physics **170**, 231 (2013), ISSN 0022-2291.

[8] H. Grundmann, A. Schilling, C. A. Marjerrison, H. A. Dabkowska, and B. D. Gaulin, Mat. Res. Bull. **48**, 3108 (2013).

[9] L. Chapon, C. Stock, P. Radaelli, and C. Martin(arXiv:0807.0877v2, accessed April 14, 2014).

[10] P. Fischer, G. Frey, M. Koch, M. Könnecke, V. Pomjakushin, J. Schefer, R. Thut, S. N., R. Bürge, U. Greuter, S. Bondt, and E. Berruyer, Physica B: Condensed Matter **276-278**, 146 (2000), ISSN 0921-4526.

[11] K.-S. Lee and M.-H. Whangbo, Inorg. Chem. **45**, 10743 (2006).

[12] M.-H. Whangbo, H.-J. Koo, and D. Dai, J. Solid State Chem. **176**, 417 (2003).

[13] P. J. Hay, J. C. Thibeault, and R. Hoffmann, J. Am. Chem. Soc. **97**, 4884 (1975).

[14] M. Kofu, J.-H. Kim, S. Ji, S.-H. Lee, H. Ueda, Y. Qiu, H.-J. Kang, M. A. Green, and Y. Ueda, Phys. Rev. Let. **102**, 037206 (2009).

[15] D. L. Quintero-Castro, B. Lake, E. M. Wheeler, A. T. M. N. Islam, T. Guidi, K. C. Rule, Z. Izaola, M. Russina, K. Kiefer, Y. Skourski, and T. Herrmannsdorfer, Phys. Rev. B **81**, 014415 (2010).

[16] I. D. Brown and D. Altermatt, Acta. Cryst. **B41**, 244 (1985).

[17] R. M. Wood, K. A. Abboud, R. C. Palenik, and G. J. Palenik, Inorg. Chem. **39**, 2065 (2000).

[18] C. Shannon, Bell Syst. Tech. J. **27**, 379 (1948).

[19] G. Radtke, A. Saul, H. A. Dabkowska, G. M. Luke, and G. A. Botton, Phys. Rev. Let. **105**, 036401 (2010).